AD-A198 051

Measurements of Atmospheric Transmission through Falling Snow

Final Report

by

Dr. A Ben-Shalom and Dr. A. D. Devir

EUROPEAN RESEARCH OFFICE

United States Army

London England

contract Number DAJA45-84-C-0008

Approved for Public Release, distribution unlimited

Report No. R.A.A/151-87 September 1987

TABLE OF CONTENTS

ABSTRACT

Measurements of atmospheric transmission during periods of snowfall were made in the infrared and the visible spectral region, during winters of 1984-1987. Two ~~companies~~ field experiments were carried out in Israel and one ~~campaign~~ [illegible] in West Germany. Results of these measurements are presented here. The measured data and results are not sufficient for validation or correction of the various models.

1 INTRODUCTION

Electro-Optical systems are significant affected by naturally occurring obscurants such as snow, rain, fog and dust. In order to properly assess these effects, basic physical processes of environment obscurants must be understood. Modeling of the environmental conditions and their effects on E-O propagation must be combined with field tests for validation and improvement of the models. The U.S. Army Research Laboratories (CRREL, ASL) have generated field tests (SNOW ONE) aimed towards an understanding of the effect of snow on the performance of military E-O systems. Much scientific information and data of significant relevance have been obtained from these tests. However, some uncertainties still exist in regions such as the forward scattering contribution to the visible and IR wavelengths; the spectral extinction dependence on wavelength ; polarization effects of snow propagation.

The EORC of the Technion has been involved during the past years, in making measurements of the transmittance in the 2.8-14 micron region, in various parts of Israel using a mobile laboratory.

The test proposal is to carry out a snow experiment in the Mideast. It is proposed to conduct spectral transmission measurements to achieve the following objectives:

a. Measure absolute spectral transmittance through falling snow in the 0.4-14 micron, with special attention to the transition region.

b. Measure the small angle forward scattered lobes at visible and IR wavelengths.

b. Provide a test-point of Mideast Climatology as a different cold region environment.

In order to address some of these objectives, a series of measurements ot atmospheric transmission in the infrared and the visible were made during the winters of 1985-1987. The instrumentation described in Chaper 2 includes devices designed and build at EORC.

2 INSTRUMENTATION

A. Location

The region chosen in Israel for snow measurements is the northern part of the Golan Heights, with average altitude of 1000m and the highest mountain is Mount Hermon (about 2000m). Graph 2.1 shows the annual statistics of snow faling days as a function of the month. From this graph it is quite clear that the highest chances for measurements of falling snow are in the months of December/January. The site for measuring falling snow was chosen as Kibutz Merom-Golan .

B. The Optical Receiver

The optical receiver shown in Fig. 2.2 is a dual-channel spectroradiometer that was developed by the Technion Infrared Radiometry Laboratory for field measurements in the visible and infrared, in the $0.3 - 14.0\mu m$ region. The need for this receiver arose from the impracticability of using existing spectroradiometers for measurements with high sensitivity in the very wide spectral range mentioned above. The design was based on the following principles:

- A flat response field-of-view over a reasonable pointing angle ($\sim$ 2mrad) is required along with a blur circle significantly smaller than the detector dimensions (2mm).

- To avoid the necessity of changing detectors for the various spectral regions, and for wide-band spectral observations, the radiation falls simultaneously on two detectors, after a 45° dichroic beam splitter.

- Spectral resolution is obtained by the use of several continuously variable filters (CVF), which cover the 0.7-14 micron range, and which are interchanged by a simple mechanical mechanism.

- A modular design is used so that changes in instrumental parameters and repairs in the field can be carried out simply.

Fig. 2.2 shows the dual-channel spectroradiometer in detail. The collecting optics are based on a 20 cm diameter f/4 spherical primary mirror. This makes the instrument about 80 cm long. The larger f-number enables aberrations to be avoided without the expense of a paraboloid, and a small field of view to be achieved easily (an essential for the experiments for which the instrument was designed). The large f-number also indicates the suitability of the Newtonians telescope principle.

After the collecting optics, the radiation passes through an optional internal chopper (400-900 Hz), and is focussed onto a field stop. The field stop is reflecting, and all light from the region around its aperture is reflected to an eyepiece with the aid of which the instrument is oriented. A set of field stops, with various sizes of aperture, is provided. The field of view (FOV) of the spectroradiometer is determined by the ratio of the field stop to the focal length of the primary mirror; usually for atmospheric transmittance measurements a FOV of 2 mrad is used.

The continuously variable filters follow the field stop and then the radiation reaches the dichroic splitter. After this, it is concentrated on the two detectors by means of AR coated ZnSe lenses.

The chopper is designed with polished blades at 45° to its axis, so that while it is closed the detectors see by reflection an internal black body at the ambient temperature, which is measured by a resistance sensor.

To cover the full range of 0.7-14 micron simultaneously, a set of two detectors InSb and HgCdTe - is used with a dichroic beam splitter which transmits wavelengths above 6 μm and reflects the rest. Each detector has its own matched preamplifier. With these cooled detectors, we have achieved the following N.E.T. (with 3% wavelength resolution and 10 msec integrating time)

at 10 micron 0.08 degree (HgCdTe)

at 4 micron 0.01 degree (InSb)

It should be noted that the internal chopper of the spectroradiometer is used only in the calibration stage, before and after each measurement of the chopped signal from the radiation source. During the measurement of the chopped signal from the radiation source the internal chopper is stopped at an open position. The detection system is then synchronously locked to the chopping frequency of the source which is transmitted via a VHF channel. The difference between the duty cycles and the first Fourier components of these two chopping frequencies (and signals) is unimportant.

The signals from the detectors are recorded and averaged by a computer which controls the position of the CVF, or the wavelength at which the measurement is taking place. As a result, a good S/N ratio is obtained even at optical paths of 11 Km in the 3-5 μm region and 24 Km in the 8-12 μm region.

C. The Radiator Source

In order to achieve the highest possible radiant intensity along the optical path of the experiment we have built a blackbody source whose radiation is collimated by Cassegrain optics. It produces a beam with an angular spread of about 10 mrad and has an exit aperture diameter of 64 cm (with the central 10% of the area obscured). The source itself is a graphite element electrically heated in a nitrogen atmosphere. It has successfully operated at 3000 K, although we generally work at 2400 K, although we generally work at 2400 K in order to increase the element lifetime, which is only about half an hour at 3000 K.

The source is illustrated schematically in Fig. 2.3. The large exist mirror is a metal parabolic reflector. It is supported in an aluminium frame around its periphery by eight screws, which are adjusted individually to reduce aberrations to a minimum. As a result a blur circle with angular diameter about 5 mrad can be achieved. The secondary hyperboloidal mirror was diamond turned from solid aluminium in accordance with a calculated profile and subsequently polished. The optical parameters were essentially dictated by the diameter and focal length of the large paraboloid as well as by the diameter of the graphite element.

In order to illuminate the exit aperture uniformly when the aberrations in the paraboloid and the magnification of the hyperbolid are taken into account, we calculated that the source needs to have a uniformly high temperature over a disc of about 5 mm diameter. Our original idea was to make an almost blackbody of these dimensions by drilling a radial hole into a hollow cylindrical graphite tube element, but it turned out that the radial hole shortened the life of the graphite element, and that the use of the outside surface of the graphite tube with no radial hole was quite satisfactory. The way in which the results are calculated in any case makes the exact emissivity unimportant. Considerable effort was put into optimizing the design of the elements as to achieve the highest possible temperature from a 6 kW a.c. supply.

The graphite element is surrounded by a radiation shield of polished aluminium. To prevent melting due to thermal deterioration and runaway of its reflectivity, the shield is cooled by running water. Immediately, outside the radiation shield is the two-bladed rotating chopper turned by an air turbine of the type used for a dental drill, which is the smallest high-speed motor available. Although the turbine is capable of much higher speeds, aerodynamic drag on the chopper dictates a highest frequency of 450 Hz.

The element operates in a stream of pure dry nitrogen, fast enough to exclude atmospheric oxygen since there are no windows in the apparatus.

At the usual working temperature of 2400 K the lifetime of a graphite element is about 3 hrs. This lifetime is somewhat shortened under windy conditions, when it becomes impossible to prevent the entrance of oxygen completely. The complete optical and electrical system was designed around the need for easy and quick dismantling into units none of which weighs more than 20 kg.

A small fraction of the chopped radiation is collected by a photodiode which is used to modulate a 10 W VHF transmitter as the reference signal for synchronous detection.

The temperature of the element is monitored with an optical pyrometer and regulated manually. Automatic regulation was considered at one time, but since the typical time-scale for detectable temperature changes is several minutes, automatization appeared to be an unnecessary complication.

The visible transmissometer consists of a 8 mW He-Ne laser source and a 3 1/2 inch diameter silicon-detector receiver. The source is chopped at a frequency of 600 Hz. An optical pick-up on the chopper wheel provides the reference signal transmitted by radio wave to the receiver station for demodulation purposes.

Snow Concentration

The falling snow was measured by standard micro balance instrument. The snow accumulates on a 30x30 cm plate area dish, after each 15 minutes it was heated and the volume of the melted water was recorded. No snow crystal characterization was made. Temperature, humidity, pressure, and wind were measured with standard meteorological instruments. The sensors were mounted near the source station and the signals were continuously recorded.

Fig. 2.1

PROBABILITY OF SNOW OCCURENCE IN ISRAEL

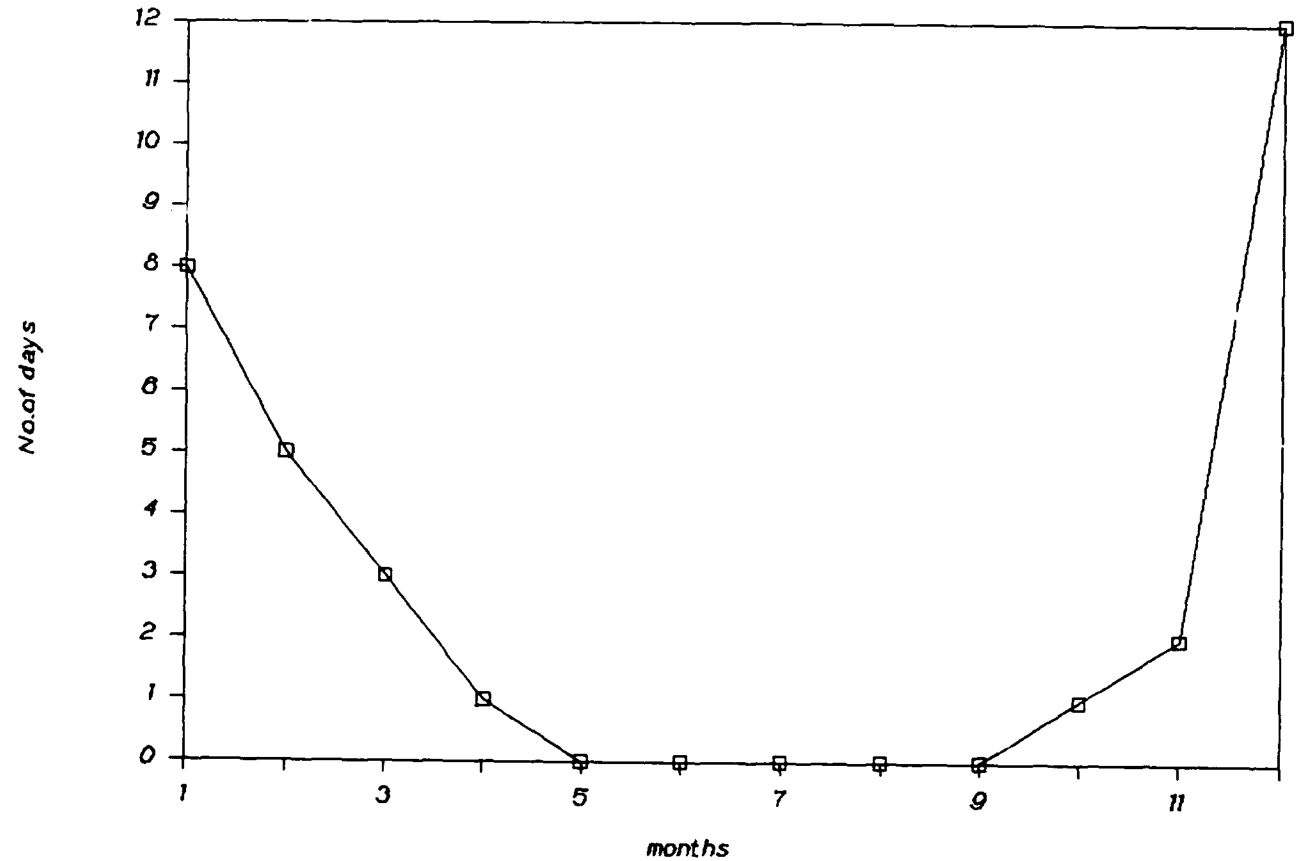

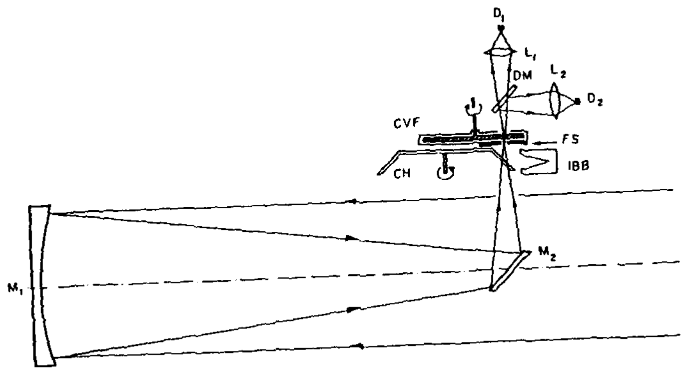

Figure 2.2 Schematic diagram of the dual-channel spectroradiometer: M_1 - primary mirror (f = 80 cm, d = 20 cm), M_2 - diagonal mirror, IBB - *internal blackbody*, CH - internal chopper, FS - field stop, CVF - circular variable filter, DM - dichroic mirror, L_1, L_2 - AR coated ZnSe lenses, D_1 - MCT detector, D_2 - InSb detector.

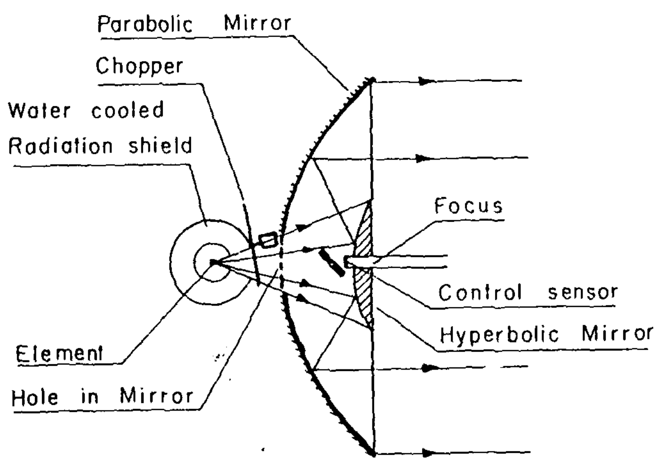

Figure 2.3 Schematic diagram of the collimated high temperature blackbody source.

3 MEASUREMENTS AND RESULTS

3.1 Winter 1984-1985

The side selected for the test was at Kibbutz Merom Golan, situated at about 1270 meter altitude on the Golan Heights.

A folded optical path was used in order to operate both the source and the receiver at the same station. The path was folded by means of retro-reflector made of 30x30 cm from surface mirrors. The retro-reflector was mounted on top of a hill (Fig. 3.1) so that the total LOS length of 1200 meters was obtained. The instrumentation was mounted in a shelter (Fig. 3.2). In Fig. 3.3 we see the 8" dia. of the receiver and the 26" dia. of the IR source. The visible transmissometer is given in Fig. 3.4. The test set-up was installed at the side on 21 Nov. 1984. The first snow storm was on 26 Dec. 1984 for about 28 hours. The falling snow was mixed with very heavy fog, visibility less than 20 meters, no measurements took place.

The second snow storm was on 27 Jan. 1984. These snow episodes started in the absence of fog with observed visibility of more than 3000 meter. The type of snow crystals observed was wet-snow (frozen water) spatial dendrites.

SUMMARY OF DATA COLLECTED ON THIS SNOW EPISODE

1984/85

Date	Time	Type	Temp	RH	VIS
			°C	%	Km
27.1.85	21:25-21:35	Snow with Rain	2.5	98	< 3
	21:35-21:50	Wet Snow	2.5	98	~ 2
	21:50-23:10	Wet Snow with Fog	2.0	98	< 0.1
	23:10-09:35	Wet Snow with Heavy Fog	1.7	48	< 0.02
28.1.85	04:35-end	Clear Atm. No Snow	3.5	98	> 5

TOTAL SNOW ACCUM = 12 mm

In Fig. 3.5 and Fig. 3.6 we present the results of this snow episode. Only the 25 minutes of wet snow (21:35-21:50) are suitable for data reduction.

The instruments were left in place and additional measurements were attempted during this winter. However, no more snow fell during the next two months, as it was an unusually warm winter, even for this location.

FIGURE 3.1 RETRO REFLECTOR LOCATION AT K. MEROM GOLAN

FIGURE 3.2 INSTRUMENTATION LOCATION; WINTER 84/85

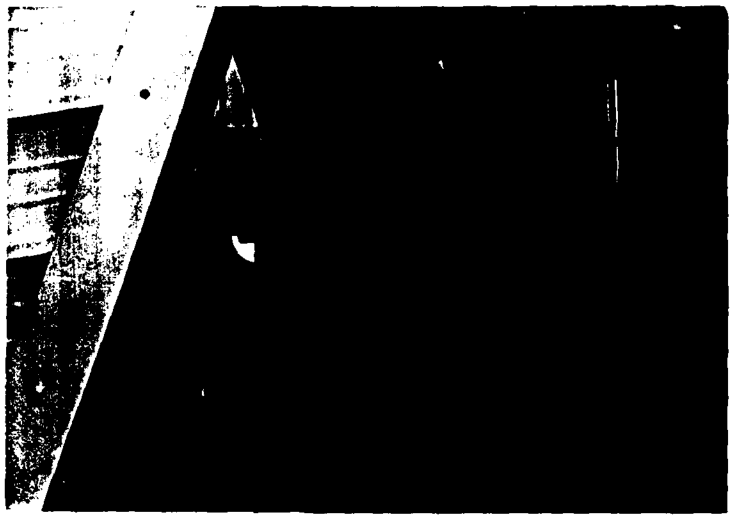

FIGURE 3.3 SOURCE AND RECEIVER;WINTER 84/85

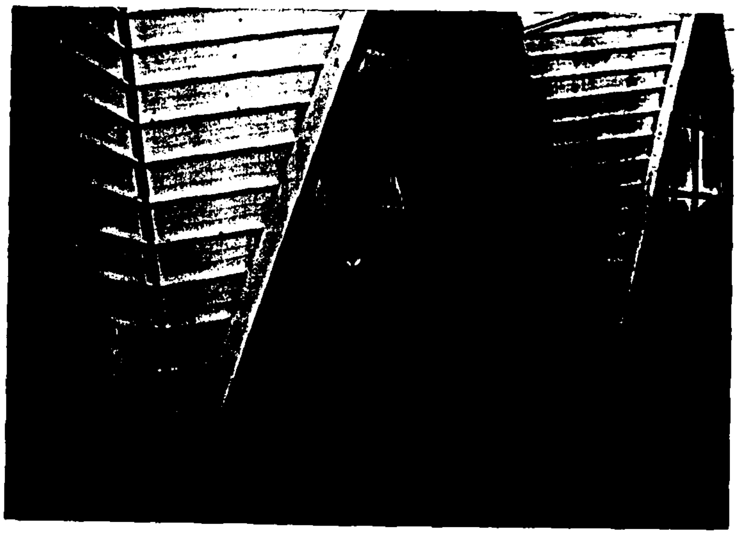

FIGURE 3.4 VISIBLE TRANSMISSOMETER; WINTER 84/85

Fig: 3.5 RAIN EQUIV.SNOW RATE 3–7 mm/hr

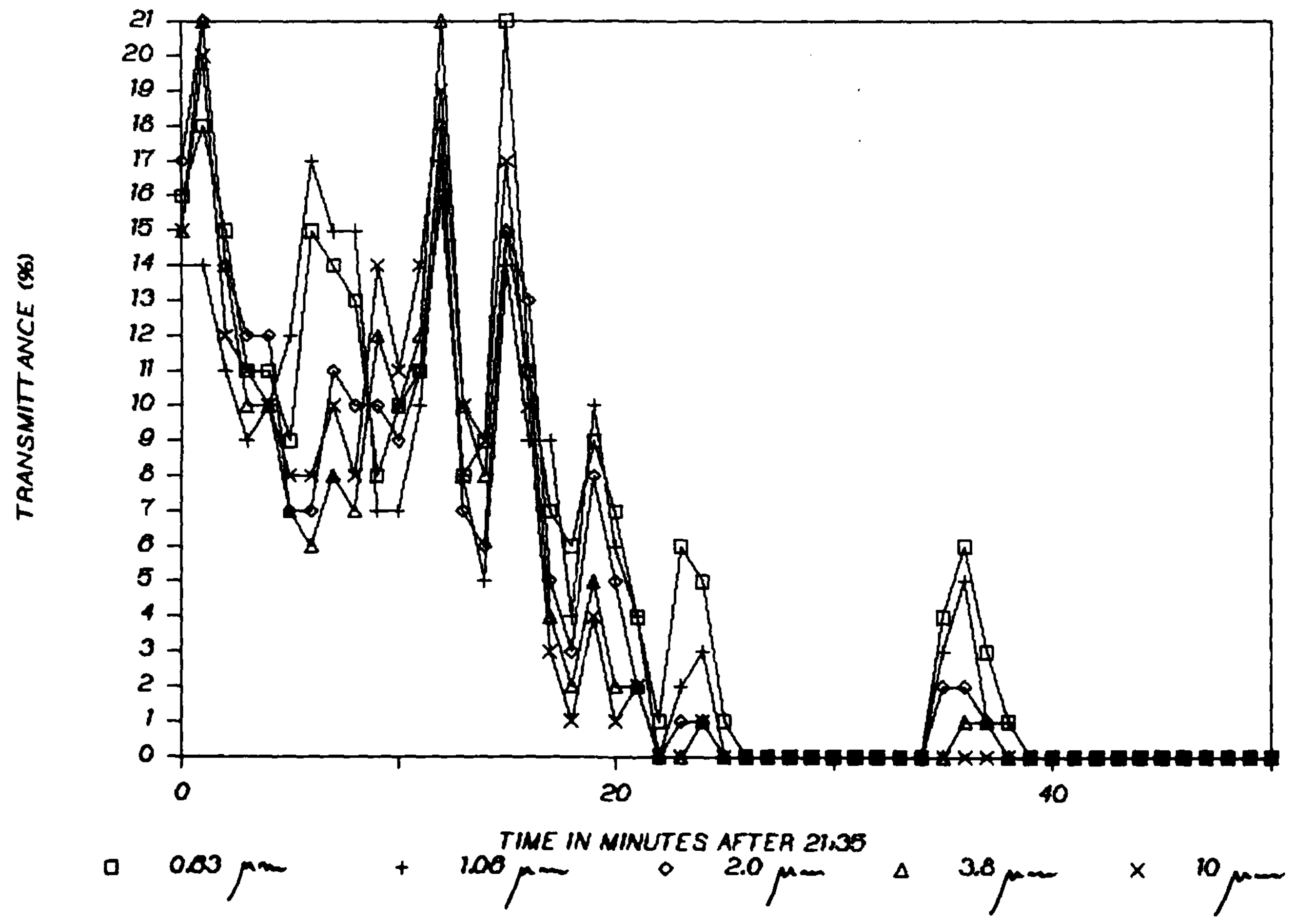

Fig: 3.6 RAIN EQUIV.SNOW RATE 3–7 mm/hr

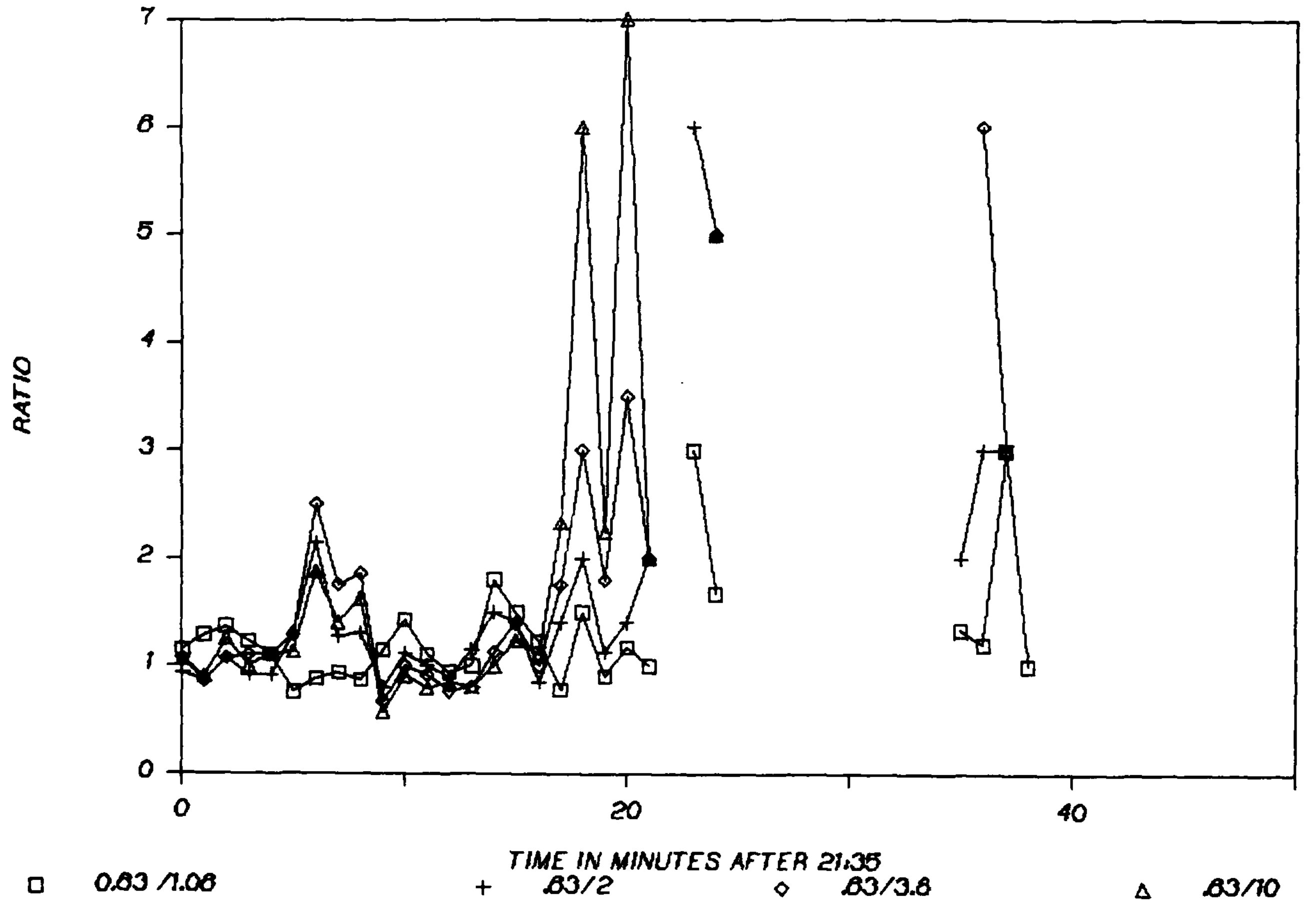

3.2 Winter 1985-1986

As a result of the first winter test, we selected a new location for our measurements, HAAR ODE m, situated at about 1480 meter altitude on the north part of the Golan Heights. The source side was in a storage shelter and the VIS/IR receives side was mobile in a VAN (Fig. 3.7). The selected range LOS was 970 meter.

The new set-up instrumentation was installed at this side on 17 Nov. 1985. The first snow storm (that was also the last one for this year) was on 21-23 Dec. 1985. The falling snow was wet snow mix with frozen drops of water.

SUMMARY OF DATA COLLECTED ON THIS SNOW EPISODE 85/86

Date	Time	Type	Temp °C	RH %	VIS Km
21.12.85	23:10-24:00	Snow, Wet	0	100	<4
22.12.85	00:00-02:30	Snow with light fog	-1	100	<2
	02:30-14:30	Snow with heavy fog	-1	100	<0.01
	14:30-19:15	Clear	+1	90	>6
23.12.85	19:15-11:30	Wet Snow with fog	0	100	<0.01

Total Snow Accum = 127 mm

In Fig. 3.8 and Fig. 3.9 we present the results of this episode.

No more snow fall with the absence of fog occurred during the rest of this winter. Because the amount of data was not sufficient, and this was the second unusually warm winter in a row, we planned to perform more measurements of falling snow in Germany, during the winter 1984-1987.

FIGURE 3.7 RECEIVER STATION; WINTER 85/86

Fig 3.8 WINTER 1985/'86

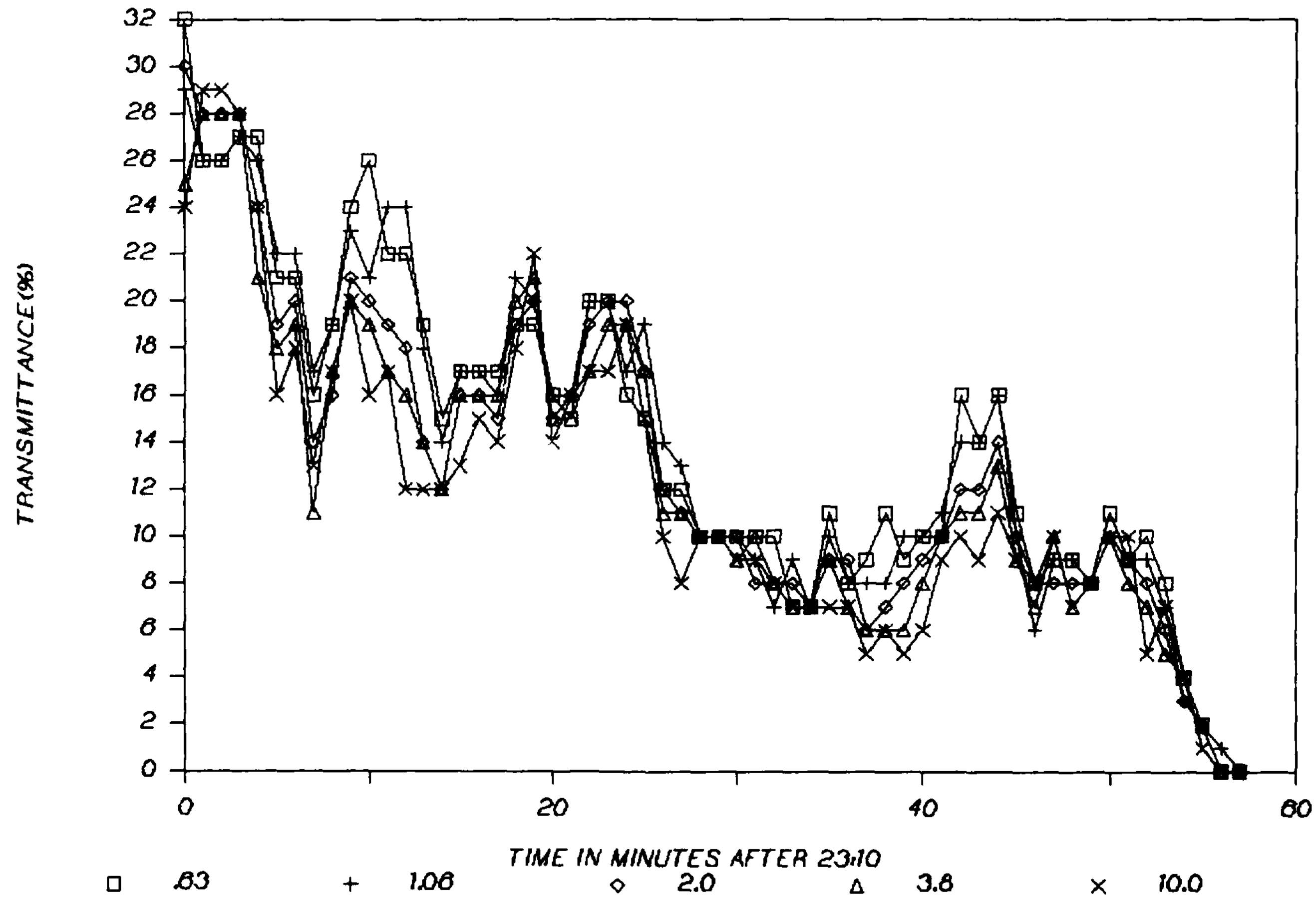

Fig 3.9 WINTER 1985/'86

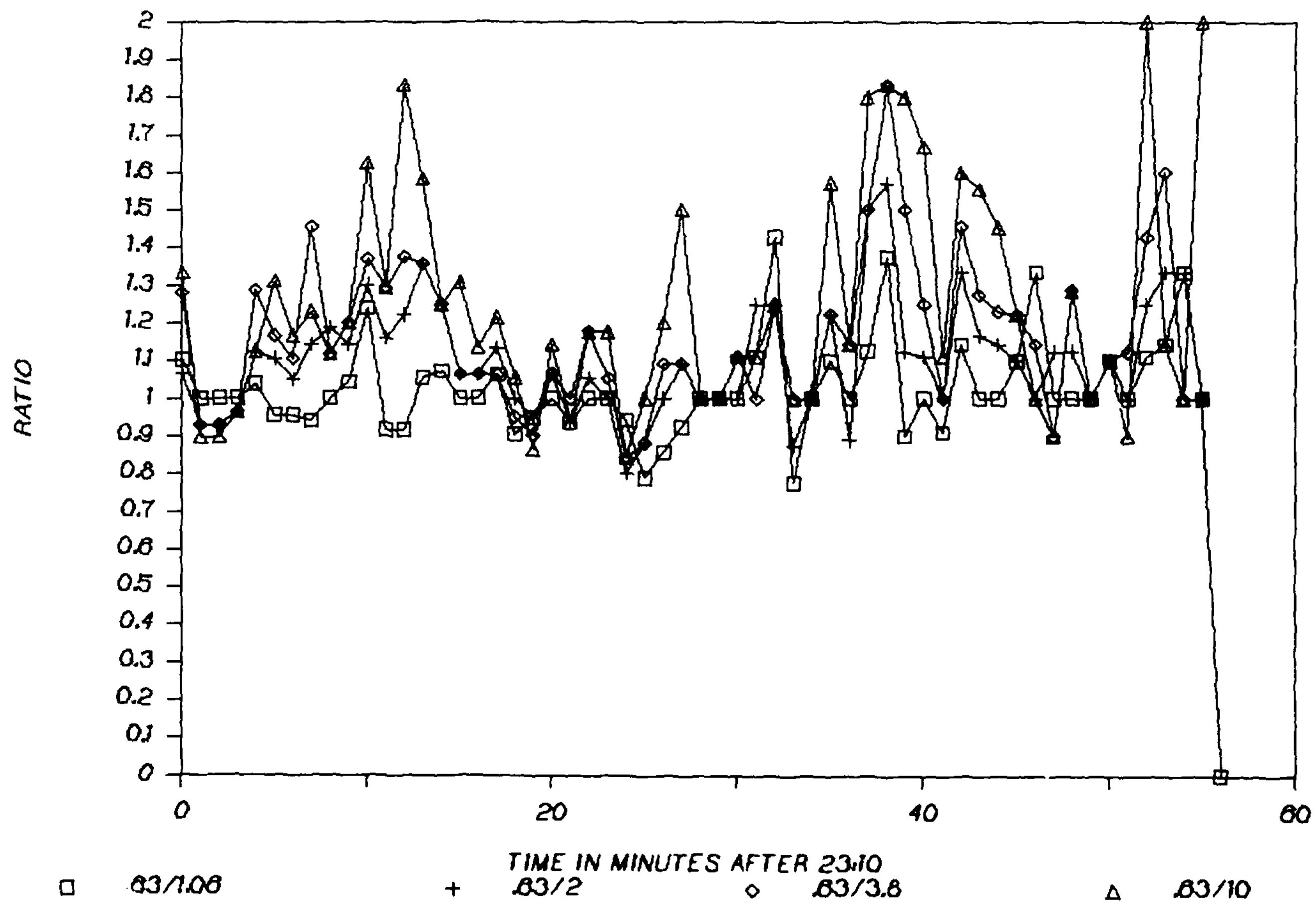

Winter 1986-1987

In view of the fact that for two consecutive winters in Irael, falling snow with no accompanying fog was not observed, it was decided to continue with the measurement program in the winter of 86/87 in Europe. After considerable efforts we got a positive response from the FFO, the German Optical Institute at Tubingen. The site selected by the FFO was an experimental side, base 52, at Bad Reichenhall, located in the South-East of Germany at an altitude of 2000m above sea level. The group leader from the FFO was Dr. A. Kohnle, who in addition to the help rendered to our program also carried out atmospheric laser scintillation experiments of the FFO. A temporary hut was erected to house the Vis/IR sources as shown in Fig. 3.10. The radiometer and accompanying instrumentation, both ours and the FFO's, were housed in a building at a distance of 695 from the source as shown in Fig. 3.11.

The experimental site was selected by the FFO based on a multi-year local snowfall record. The equipment was shipped to Germany in October '86 and subsequently placed on the mountain site. A number of absolute atmospheric spectral transmittance measurements were carried out over path lengths of several kilometers. In the period between 1/10/86 to 2/14/87 a number of measurements were carried out both by the Israeli and German groups. Appendix A contains raw data of the FFO in the visible, 3-5 and 8-12 micron spectral regions. Though there was considerable amount of snowfall (around 300 cm altogether), the accompanying fog or low level clouds restricted the visibility range to a few tens of meters only. Consequently, this did not allow us to perform systematic transmittance measurements through falling snow only. Most of the days when there was no snow the visibility was above 40km. This was ideal for other measurements as listed below using the same equipment.

a) Atmospheric transmittance measurements in the 8-12 micron region over horizontal path lengths of 4, 8, 17 and 24 kilometers.

b) Spectral radiance measurements of the natural snow background in the 0.7-13 micron region. These background results are useful for remote sensing analysis in the infrared and thermal regions. Raw spectral background data and back scattered data from a snow cloud are shown in Fig's 3.13 and 3.14. All these measurements will be published in a separate report since they are not part of the main program.

FIGURE 3.10 SOURCE AND RECEIVER IN THE SOURCE LOCATION; WINTER 86/87

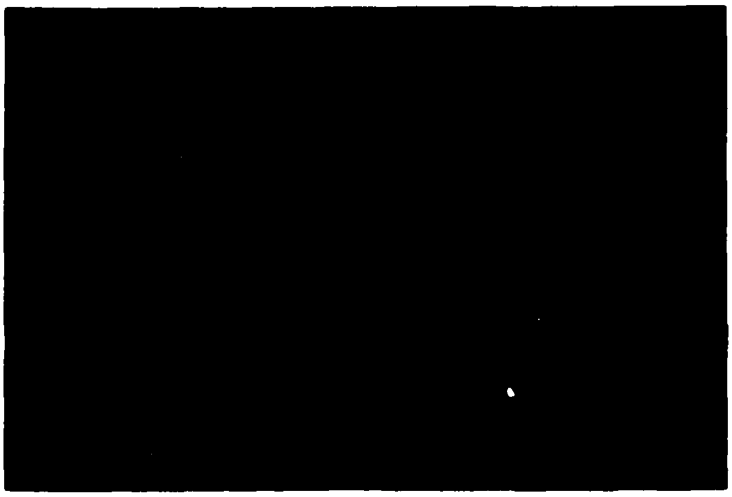

FIGURE 3.11 RECEIVER LOCATION ; WINTER 86/87

Fig 3.12

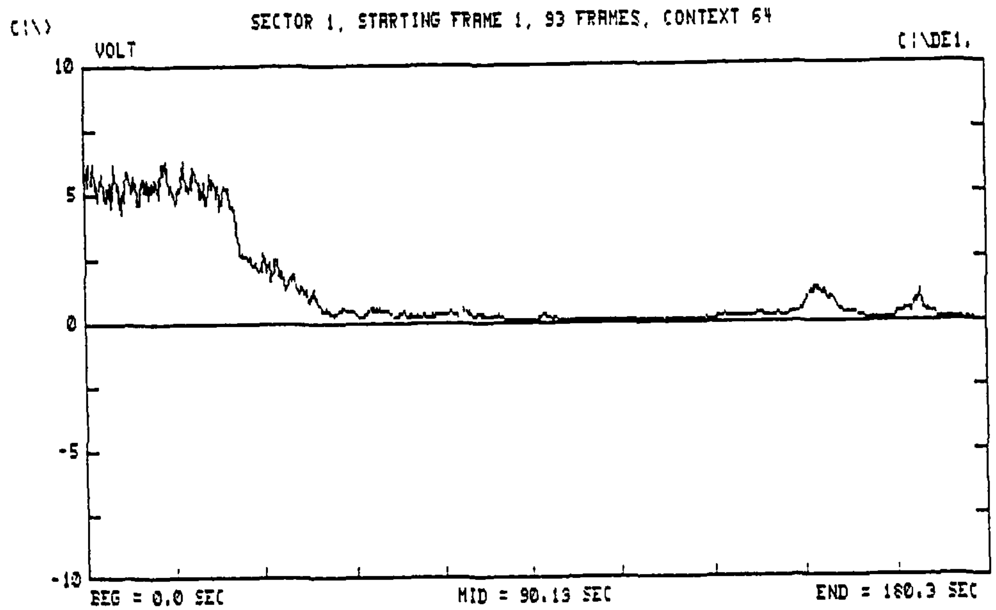

27 / ITR 2

Fig. 3.13

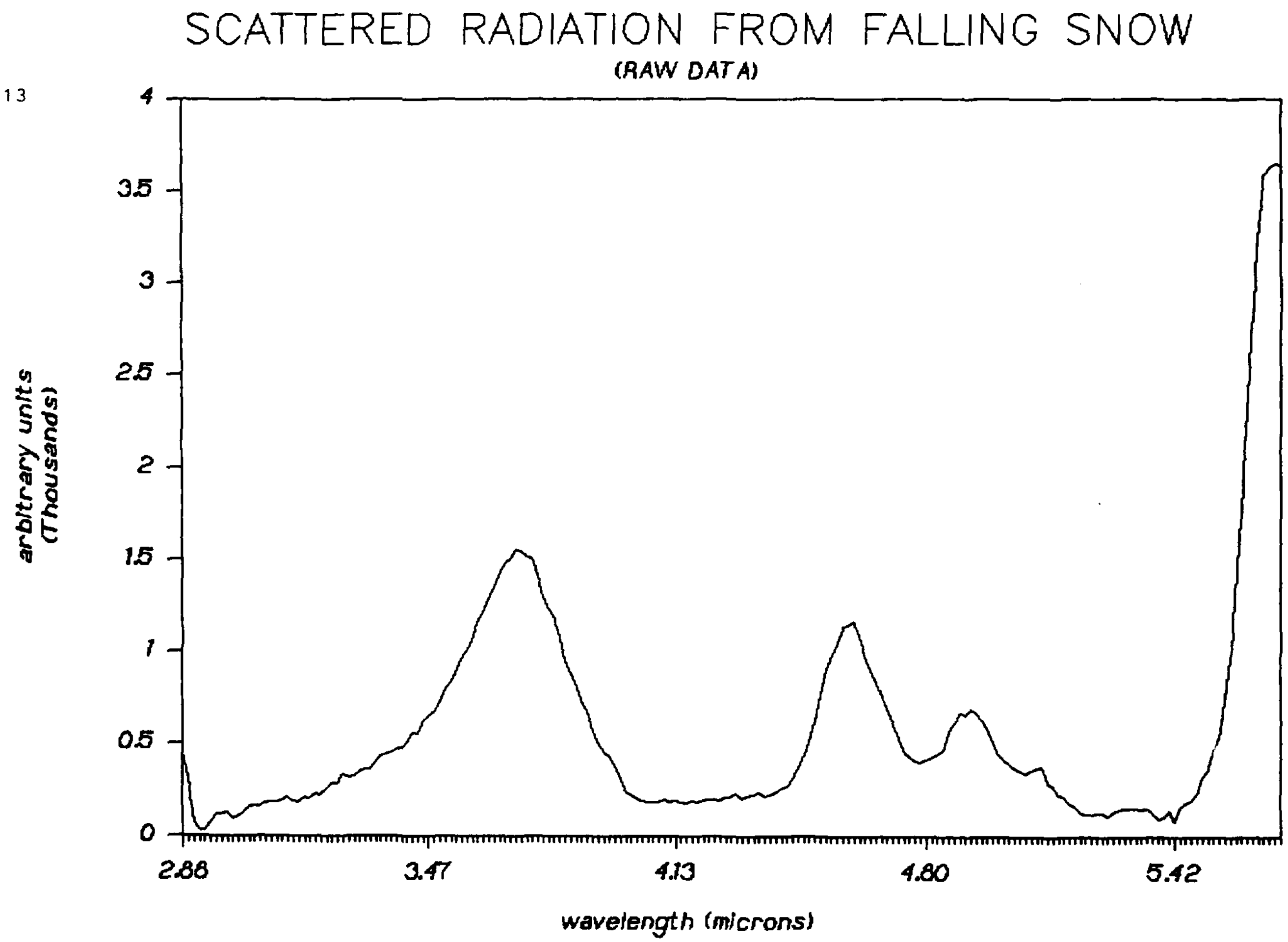
SCATTERED RADIATION FROM FALLING SNOW
(RAW DATA)
arbitrary units
(Thousands)
4
3.5
3
2.5
2
1.5
1
0.5
0
2.86
3.47
4.13
4.80
5.42
wavelength (microns)

Fig 3.14

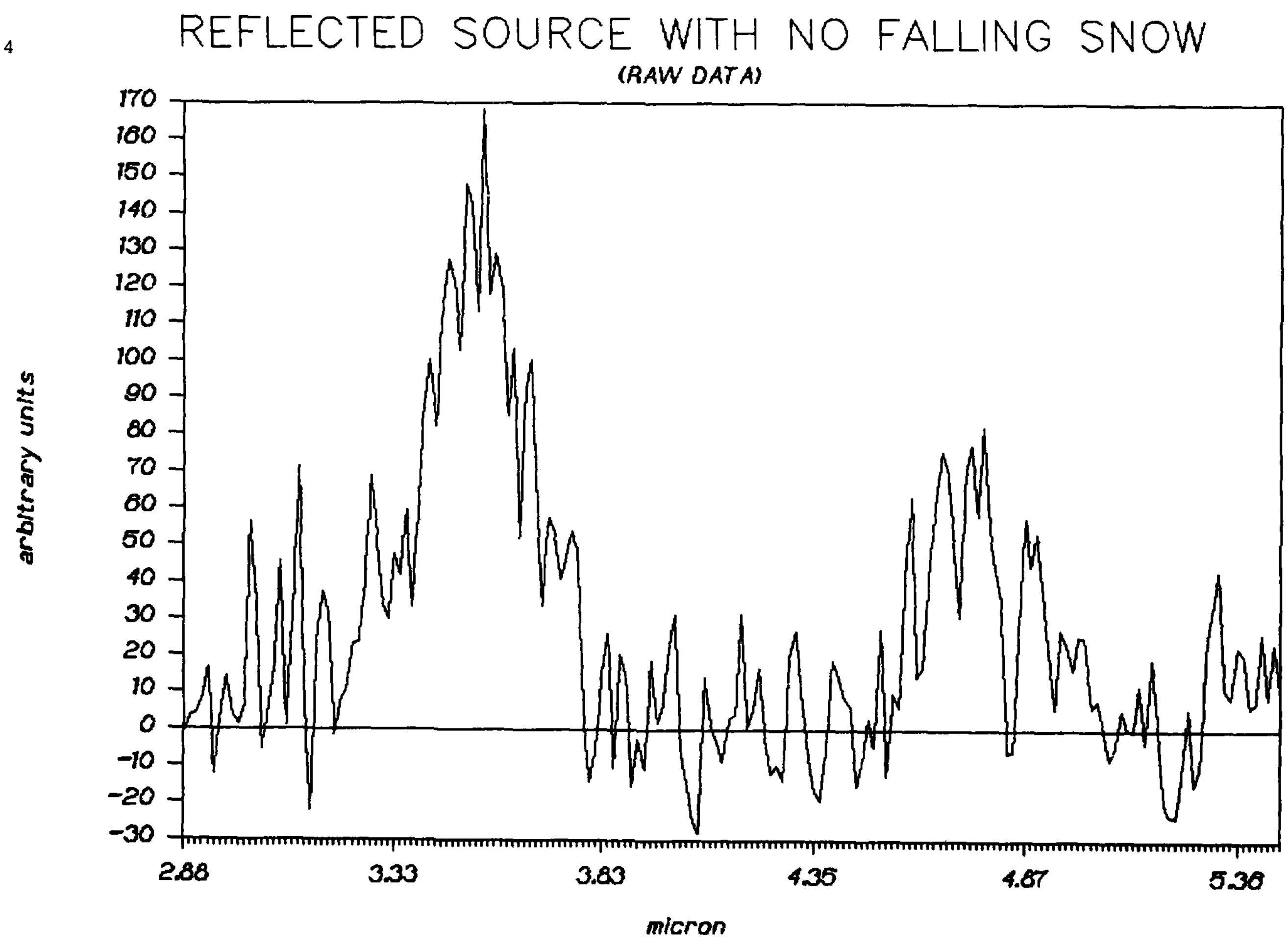
REFLECTED SOURCE WITH NO FALLING SNOW
(RAW DATA)
arbitrary units
170
160
150
140
130
120
110
100
90
80
70
60
50
40
30
20
10
0
-10
-20
-30
2.88
3.33
3.83
4.35
4.87
5.36
micron

3.4 Spectral Reflectance

The set-up for measuring spectral reflectance and absolute calibration is given in Appendix B. Snow samples were gathered into thermally isolated containers and transferred in 3 hours to the laboratory for measurement.

The snow was new, wet and mixed with refrozen water drops.

The reflectance of dry snow is high at wavelengths below $1.4\mu m$, owing to the small molecular absorption of ice and multiple scattering of radiation in snow. At wavelengths above $1.4\mu m$, the strong absorption of ice reduces the reflectance of snow typically to a few percent. In Fig. 3.15 we present the results of 4 different samples. From the sharp reduce reflectance value around $1.2\mu m$ we see effect of the molecular absorption of water and ice.

Fig 3.15

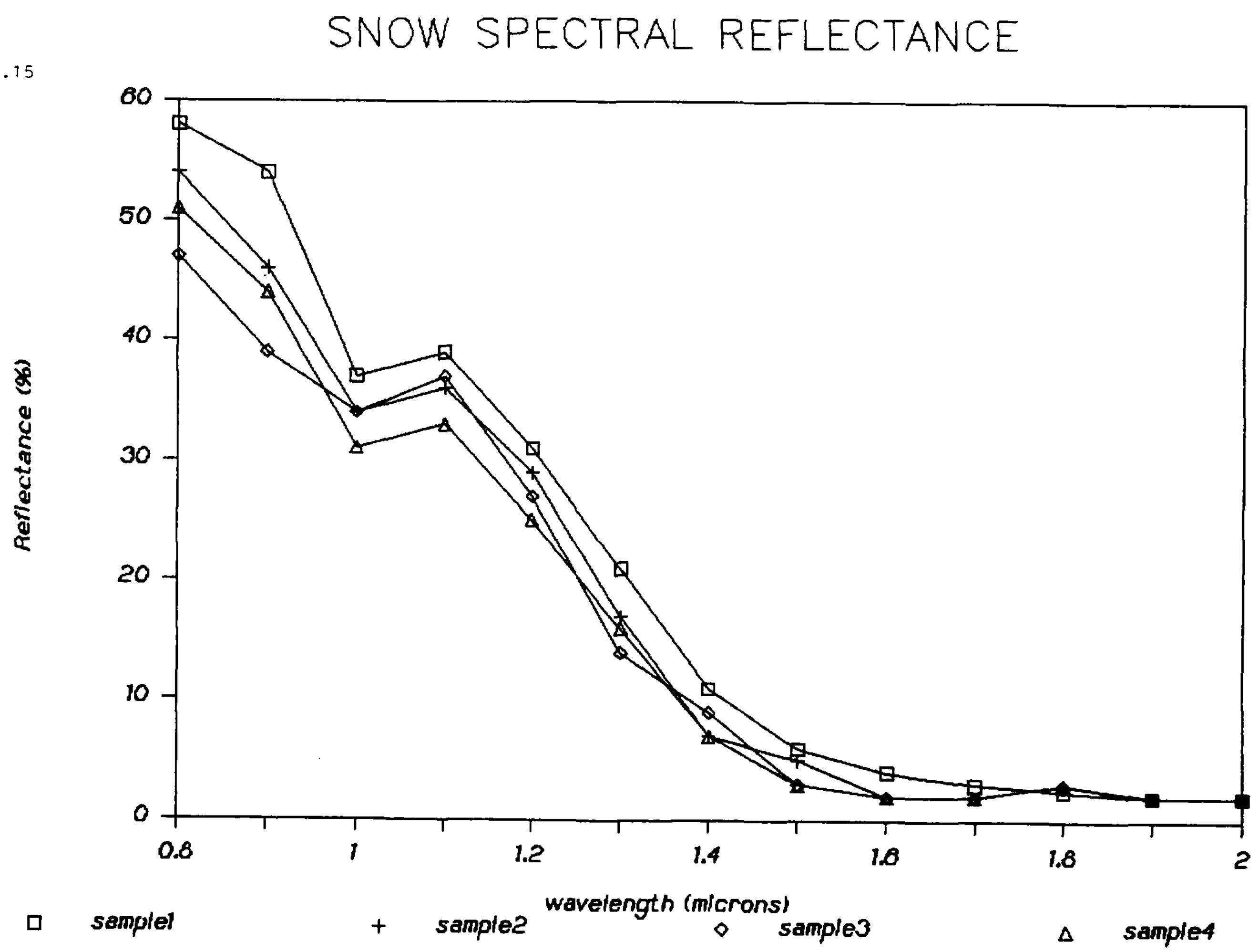
SNOW SPECTRAL REFLECTANCE
Reflectance (%)
0
10
20
30
40
50
60
0.8
1
1.2
1.4
1.6
1.8
2
wavelength (microns)
sample1
sample2
sample3
sample4

4. Conclusions

The main conclusions are as follows:

A) In Israel falling snow is invariably accompanied with fog that limits visibility to a few tens of meters only. The snow is comprised of frozen rain drops and is wet.

B) In order to perform transmittance measurements, good visibility (more than 500m) and dry snow that falls for a few hours at least are required. These conditions were not realized both in Israel and in Germany. Consequently the measured results are not sufficient for validation or correction of the predictions of various models.

C) In the future it is recommended that these experiments be carried out in regions where the probability of occurrence of appropriate snowfall and good visibility conditions is high. Also since in these experiments the expenses were considerably above the planned budget it is not possible to continue to carry out these measurements in Israel.

5. Acknowledgement

The experiment was designed to give results that validate information on the transmittance of radiation through falling snow in the Middle East. In spite of the efforts put in by us here in Israel the experiment was not a success in achieving its goals due to the meteorological conditions that prevailed in the winters of 84-86. We gratefully thank Kibbutz Marom Golan and Har Odem for the help rendered on the experimental site. The experiments at the site in Germany also failed to achieve its goals once again due to the prevailing meteorological conditions at the time of the experiments. However, we gratefully thank Dr. A. Khonle and his group from FFO for their efforts in helping us at Bad Reichenhall during the winter of 86/87. We would also like to thank the EORC for the financial help given for carrying out the experiments in Germany. Finally, we would also like to thank the U.S. Army Atmospheric Science Laboratory and the U.S. Army European Research Office (UK-London) for the support given to this program.

APPENDIX A

Raw Date from FFO

Winter 1986/1987

ELSE

Messung Nummer : 27
FfO-Filename : Mi 100
Datum : 28.1.1987
Messbeginn : 11:56
Messzeit : 180 s
Abtastrate : 100 Hz
Messort : Reiteralpe Tal WTD52 Hochberg Steige
Messentfernung : 695 m

Bereich : IR2 8-12µm X
IR1 3- 5µm
VIS Ø 650nm
Scan 2.5-15µm

Meteorologie

TT (°C)	RF (%)	FF ($m \cdot s^{-1}$)	DD (0..360°)	Q+ ($W \cdot m^{-2}$)	Q- ($W \cdot m^{-2}$)	RR ($mm \cdot h^{-1}$)	VN (km)
-5	91	3	270(W)	100	75		6

Kommentar Stark aufgewirbeltes Schneetreiben
bei starkem Wind.

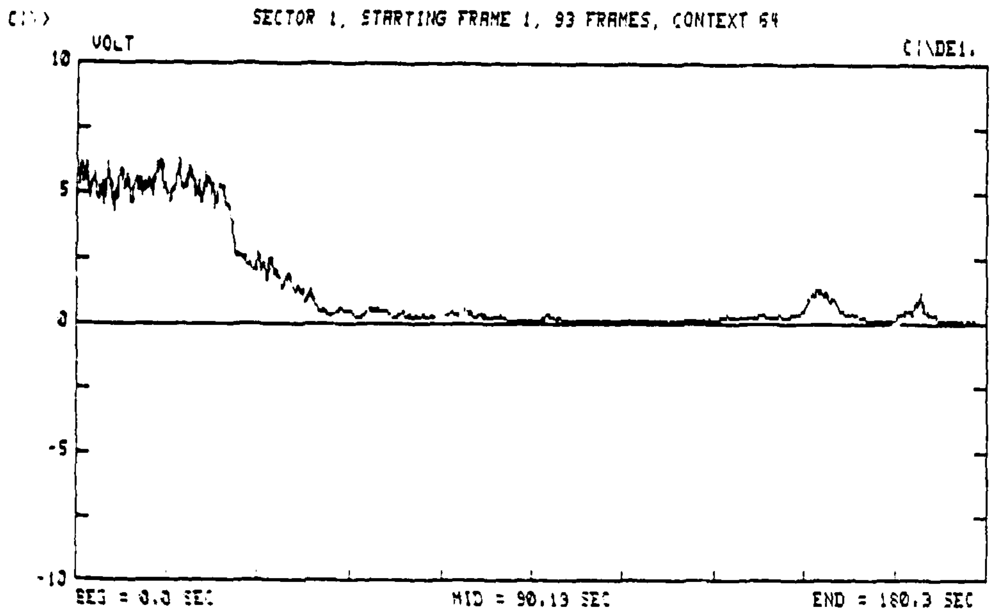
SECTOR 1, STARTING FRAME 1, 93 FRAMES, CONTEXT 64
VOLT
C:\DE1.
10
5
0
-5
-10
BEG = 0.0 SEC
MID = 90.13 SEC
END = 180.3 SEC

27 / IR 2

ELSE

Messung Nummer : 27
Ff0-Filename : Mi 100
Datum : 28.1.1997
Messbeginn : 11:56
Messzeit : 180 s
Abtastrate : 100 Hz
Messort : Reiteralpe Tal WTD52 Hochberg Steige
Messentfernung : 695 m

Bereich : IR2 8-12µm
IR1 3- 5µm X
VIS Ø 650nm
Scan 2.5-15µm

Meteorologie

TT (°C)	RF (%)	FF ($m \cdot s^{-1}$)	DD (0‥360°)	Q+ ($W \cdot m^{-2}$)	Q- ($W \cdot m^{-2}$)	RR ($mm \cdot h^{-1}$)	VN (km)
-5	91	3	270 (W)	100	75		6

Kommentar: Stark aufgewirbeltes Schneetreiben bei starkem Wind.

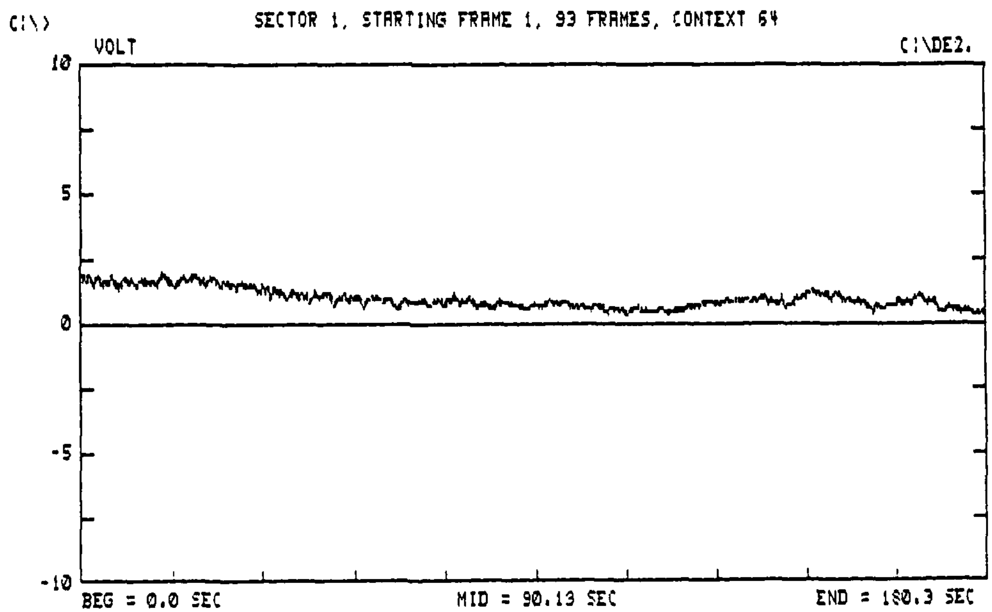
C:\>
SECTOR 1, STARTING FRAME 1, 93 FRAMES, CONTEXT 64
VOLT
C:\DE2.
10
5
0
-5
-10
BEG = 0.0 SEC
MID = 90.13 SEC
END = 180.3 SEC

- 4 -

27/17/1

ELSE

Messung Nummer : 27
FfO-Filename : Mi 100
Datum : 28.1.1987
Messbeginn : 11:56
Messzeit : 180 s
Abtastrate : 100 Hz
Messort : Reiteralpe Tal WTD52 Hochberg Steige
Messentfernung : 695 m

Bereich : IR2 8-12µm
IR1 3- 5µm
VIS Ø 650nm X
Scan 2.5-15µm

Meteorologie

TT (°C)	RF (%)	FF ($m \cdot s^{-1}$)	DD (0··360°)	Q+ ($W \cdot m^{-2}$)	Q- ($W \cdot m^{-2}$)	RR ($mm \cdot h^{-1}$)	VN (km)
-5	91	3	270(W)	100	75		6

Kommentar: Stark aufgewirbeltes Schneetreiben bei starkem Wind.

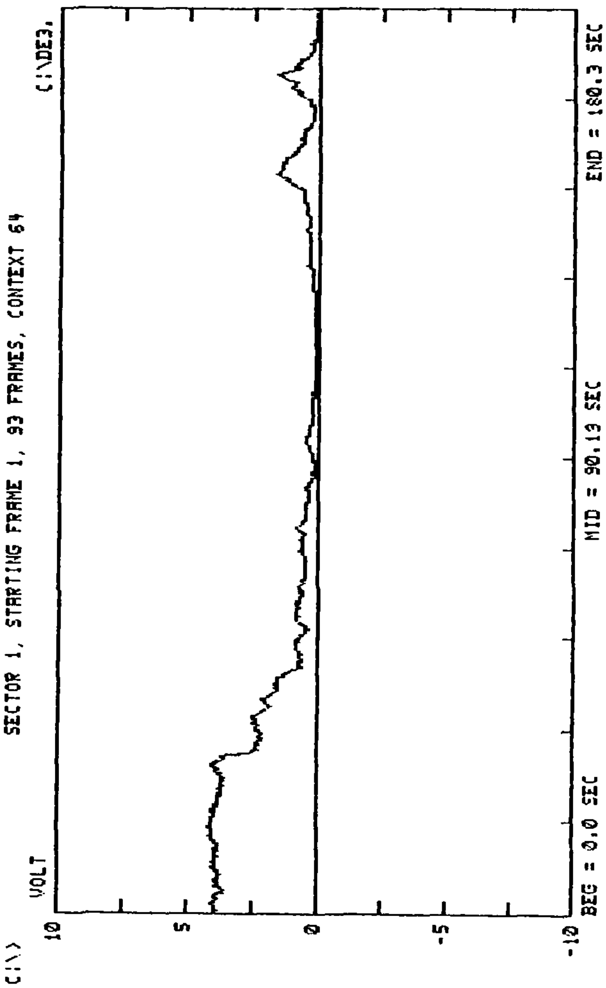
SECTOR 1, STARTING FRAME 1, 93 FRAMES, CONTEXT 64
C:\DE3.
C:\>
VOLT
10
5
0
-5
-10
BEG = 0.0 SEC
MID = 90.13 SEC
END = 180.3 SEC

ELSE

Messung Nummer : 28
FfO-Filename : Do 100
Datum : 29.1.1987
Messbeginn : 10:34
Messzeit : 3600 s
Abtastrate : 100 Hz
Messort : Reiteralpe Tal WTD52 Hochberg Steige
Messentfernung : 695 m

Bereich : IR2 8-12µm X
IR1 3- 5µm
VIS Ø 650nm
Scan 2.5-15µm

Meteorologie

TT (°C)	RF (%)	FF ($m \cdot s^{-1}$)	DD (0··360°)	Q+ ($W \cdot m^{-2}$)	Q- ($W \cdot m^{-2}$)	RR ($mm \cdot h^{-1}$)	VN (km)
−10	87	1	290	200	120		>10

Kommentar: Schneetreiben zu Beginn mit Nebel.
Dann Sonne und klar.

2.

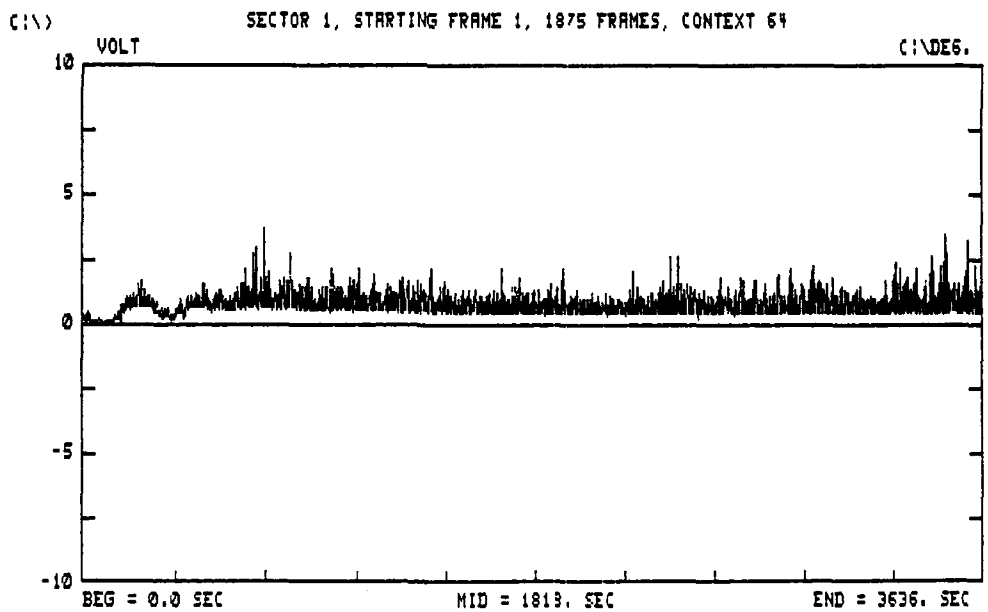
SECTOR 1, STARTING FRAME 1, 1875 FRAMES, CONTEXT 64
C:\)
VOLT
C:\DEG.
10
5
0
-5
-10
BEG = 0.0 SEC
MID = 1818. SEC
END = 3636. SEC

28/1R2

ELSE

Messung Nummer : 28
Ff0-Filename : Do 100
Datum : 29.1.1987
Messbeginn : 10:34
Messzeit : 3600 s
Abtastrate : 100 Hz
Messort : Reiteralpe Tal WTD52 Hochberg Steige
Messentfernung : 695 m

Bereich : IR2 8-12µm
IR1 3- 5µm X
VIS Ø 650nm
Scan 2.5-15µm

Meteorologie

TT (°C)	RF (%)	FF ($m \cdot s^{-1}$)	DD (0··360°)	Q+ ($W \cdot m^{-2}$)	Q- ($W \cdot m^{-2}$)	RR ($mm \cdot h^{-1}$)	VN (km)
−10	87	1	290	200	120		>10

Kommentar Schneetreiben zu Beginn mit Nebel.
Dann Sonne und klar

2.

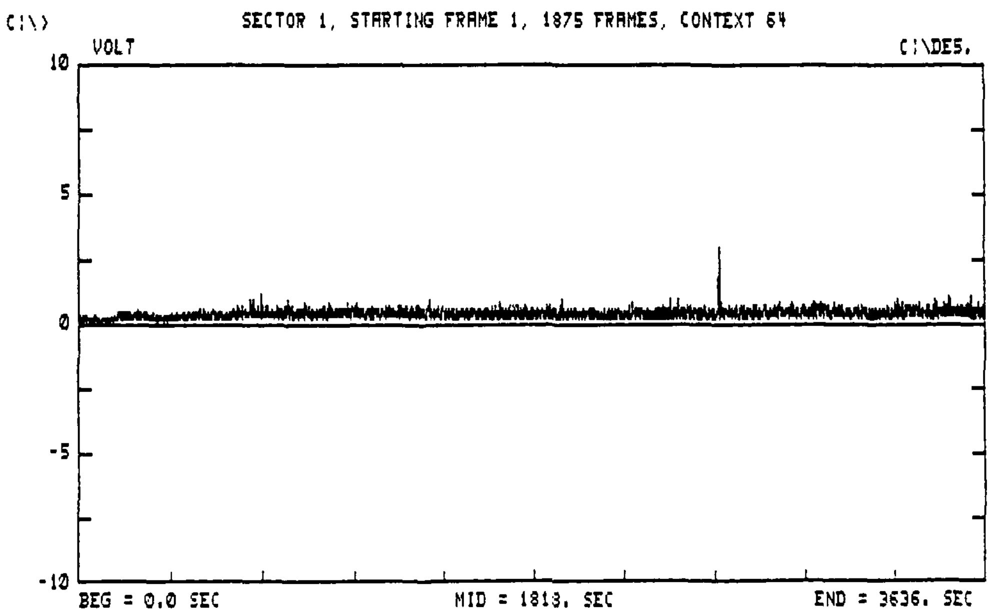
C:\>
SECTOR 1, STARTING FRAME 1, 1875 FRAMES, CONTEXT 64
VOLT
C:\DES.
10
5
0
-5
-10
BEG = 0.0 SEC
MID = 1813. SEC
END = 3636. SEC

28/1R.1

ELSE

Messung Nummer : 28

FfO-Filename : Do100

Datum : 29.1.1987

Messbeginn : 10:34

Messzeit : 3600 s

Abtastrate : 100 Hz

Messort : <u>Reiteralpe</u> Tal WTD52 Hochberg Steige

Messentfernung : 695 m

Bereich : IR2 8-12µm
IR1 3- 5µm
VIS Ø 650nm X
Scan 2.5-15µm

Meteorologie

TT (°C)	RF (%)	FF ($m \cdot s^{-1}$)	DD (0··360°)	Q+ ($W \cdot m^{-2}$)	Q- ($W \cdot m^{-2}$)	RR ($mm \cdot h^{-1}$)	VN (km)
-10	87	1	290	200	120		>10

Kommentar

Schneetreiben zu Beginn mit Nebel, dann Sonne und klar.

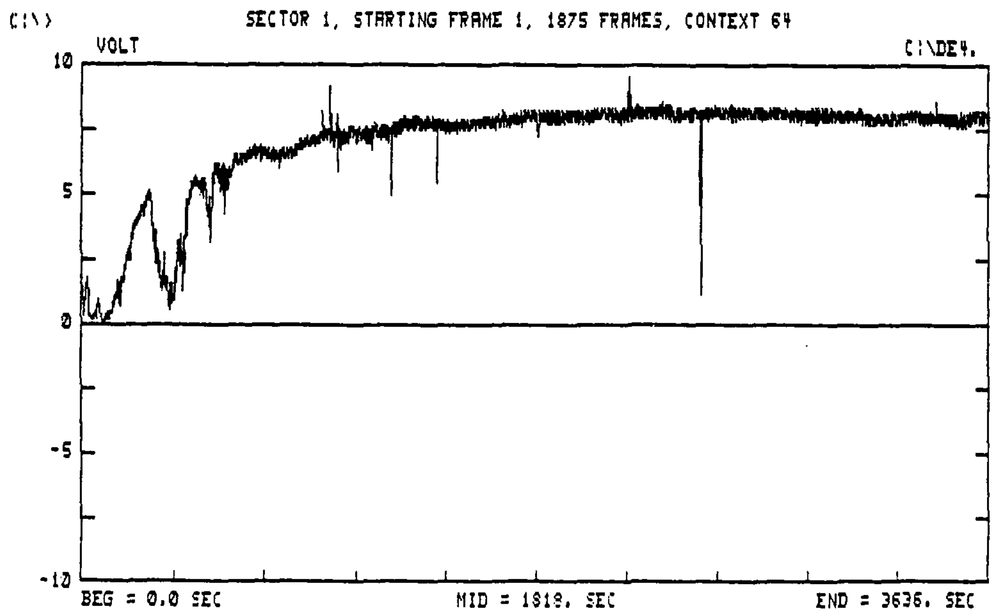

C:\>
SECTOR 1, STARTING FRAME 1, 1875 FRAMES, CONTEXT 64
VOLT
C:\DE4.
10
5
0
-5
-10
BEG = 0.0 SEC
MID = 1818. SEC
END = 3636. SEC

ELSE

Messung Nummer : 29
FfO-Filename : Do 101
Datum : 29.1.87
Messbeginn : 12:09
Messzeit : 180 s
Abtastrate : 100 Hz
Messort : Reiteralpe Tal WTD52 Hochberg Steige
Messentfernung : 695 m

Bereich : IR2 8-12µm X
IR1 3- 5µm
VIS Ø 650nm
Scan 2.5-15µm

Meteorologie

TT (°C)	RF (%)	FF ($m \cdot s^{-1}$)	DD (0..360°)	Q+ ($W \cdot m^{-2}$)	Q- ($W \cdot m^{-2}$)	RR ($mm \cdot h^{-1}$)	VN (km)
-11	87	~0	290	100	80		>10

Kommentar Gute Sicht bei klarer Sonne.

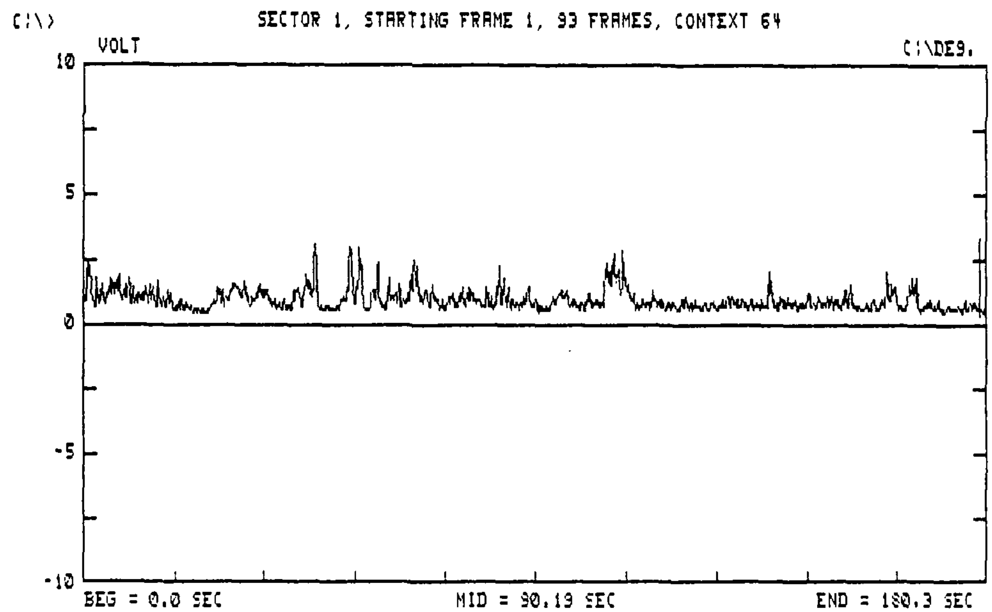
C:\>
SECTOR 1, STARTING FRAME 1, 93 FRAMES, CONTEXT 64
VOLT
C:\DE9.
10
5
0
-5
-10
BEG = 0.0 SEC
MID = 90.19 SEC
END = 180.3 SEC

29/IR2

ELSE

Messung Nummer : 29

FfO-Filename : D0101

Datum : 29.1.1987

Messbeginn : 12:09

Messzeit : 180 s

Abtastrate : 100 Hz

Messort : Reiteralpe Tal WTD52 Hochberg Steige

Messentfernung : 695 m

Bereich : IR2 8-12μm

IR1 3- 5μm X

VIS Ø 650nm

Scan 2.5-15μm

Meteorologie

TT (°C)	RF (%)	FF ($m \cdot s^{-1}$)	DD (0..360°)	Q+ ($W \cdot m^{-2}$)	Q- ($W \cdot m^{-2}$)	RR ($mm \cdot h^{-1}$)	VN (km)
−11	87	~0	290	100	80		>10

Kommentar Gute Sicht bei klarer Sonne.

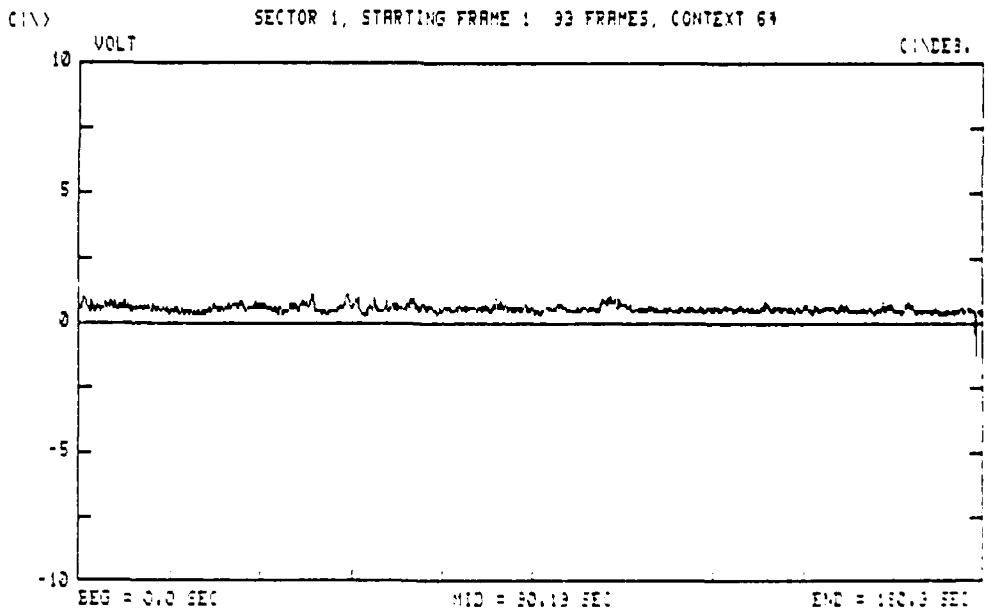
C:\>
SECTOR 1, STARTING FRAME 1 33 FRAMES, CONTEXT 64
VOLT
10
5
0
-5
-10
BEG = 0.0 SEC
MID = 80.13 SEC
END = 160.3 SEC

APPENDIX B

Spectral reflectance measuring set-up

Absolute reflectometer for the 0.8–2.5-μm region

Dan Sheffer, Uri P. Oppenheim, Dieter Clement, and Adam D. Devir

A reflectometer based on an integrating sphere operating in the 0.8–2.5-μm region is described. The reflectometer is of the absolute type and does not need a standard diffuse reflecting surface to obtain absolute reflectance values. The system is fully automatic, using computer-controlled circular variable filters as monochromators. Results for $BaSO_4$ in the region between the visible and 2.5 μm show considerable deviations from the accepted values of reflectivity for this substance.

I. Introduction

The problem of measuring reflectance of surfaces and objects is not new. Over the years many reflectometers have been built and described in the literature. However, few reflectometers are of the absolute type and fewer still operate in the infrared. Most reflectometers use an integrating sphere to carry out diffuse reflectance measurements.[1,2] The disadvantage of the relative type of reflectometer is that a standard of known reflectance is required. This standard has to be stable both chemically and optically over long periods of time. Several well-known standards for the visible have become established such as $BaSO_4$ powder or $BaSO_4$ paint and various types of opal glass. However, without the possibility of recalibration in the laboratory, the user is never certain if the standard has retained its original reflectivity. An absolute reflectometer is therefore called for, yet only few of these exist and these operate mostly in the visible.

While several absolute measurements have been published for standards such as $BaSO_4$ in the 0.8–3-μm region, there is considerable disagreement between results. The situation is even worse in the 3–14-μm region, where hardly any absolute measurements exist. Very few absolute reflectometers have been reported in the literature[3-7] and these operate mostly in the visible. This paper describes an absolute reflectometer for the region between 0.4 and 2.5 μm and a future study will deal with a similar instrument operating in the 3–14-μm region.

The authors are with Technion–Israel Institute of Technology, Physics Department, Haifa 32000, Israel.

Received 12 July 1986.

0003-6935/87/030583-04$02.00/0.

In this paper we use the abbreviations VIS for the 0.4–0.8-μm region, NIR for the 0.8- and 2.5-μm region, and FIR for the 3–14-μm region.

II. General Description of the Optical System

The system consists of several interchangeable sources, circular variable filters (CVFs), integrating spheres, and detectors. By making various combinations of these elements the operator can choose different wavelength regions for measurement. In what follows a description of each of these combinations is given.

Figure 1 shows the system operating in the visible region, using lenses and mirrors and operating by use of the substitution method.[8] Lens L_1 images the source on a CVF (manufactured by Optical Coatings Laboratories) operating in the VIS, after being chopped at 13 Hz. Lens L_2 forms a secondary image on the inner wall of the integrating sphere with the help of mirror M_2. The wall of the sphere is coated with Eastman White Reflectance Coating, catalog No. 6080, obtained from Eastman Kodak Co. To form this inner reflecting surface, ten coatings of this material, consisting of $BaSO_4$ in a binder, were applied to the inner wall of the sphere. The optical configuration of the sample was 30°/d (i.e., an angle of incidence of 30° reflected into a hemisphere). The source was a 40-W head lamp and the detector was a silicon diode. The signal was amplified by a lock-in amplifier and fed into a BBC microcomputer for data analysis. The computer also controlled the measurement procedure.

Figure 2 shows the system used in the NIR and FIR. Here only mirrors were used in the imaging system. By tilting mirrors M_5 and M_7 the NIR or the FIR could be selected, while at the same time the appropriate CVF was introduced by the operator. The two CVFs were situated on a horizontal rail which allowed moving either CVF into the beam by a simple (manual) translation. The FIR region was operated in a 45°/d configuration, using the substitution method. The

Unclassified

SECURITY CLASSIFICATION OF THIS PAGE

REPORT DOCUMENTATION PAGE

Form Approved
OMB No 0704-0188
Exp Date Jun 30, 1986

1a. REPORT SECURITY CLASSIFICATION Unclassified	1b. RESTRICTIVE MARKINGS
2a. SECURITY CLASSIFICATION AUTHORITY 2b. DECLASSIFICATION/DOWNGRADING SCHEDULE	3. DISTRIBUTION/AVAILABILITY OF REPORT Approved for public release; distribution unlimited.
4. PERFORMING ORGANIZATION REPORT NUMBER(S) Report No. R.A.A./151-87	5. MONITORING ORGANIZATION REPORT NUMBER(S) R&D 4488-EN-01
6a. NAME OF PERFORMING ORGANIZATION Technion - Israel Institute of Technology 6b. OFFICE SYMBOL (If applicable)	7a. NAME OF MONITORING ORGANIZATION USARDSG-UK
6c. ADDRESS (City, State, and ZIP Code) Senate House, Technion City Haifa, Israel	7b. ADDRESS (City, State, and ZIP Code) Box 65 FPO NY 09510-1500
8a. NAME OF FUNDING/SPONSORING ORGANIZATION U.S. ARMY Atmospheric Science Laboratory 8b. OFFICE SYMBOL (If applicable)	9. PROCUREMENT INSTRUMENT IDENTIFICATION NUMBER DAJA45-84-C-0008
8c. ADDRESS (City, State, and ZIP Code) White Sands Missile Range, NM 88002	10. SOURCE OF FUNDING NUMBERS PROGRAM ELEMENT NO. 61102A PROJECT NO. 1L161102BH57 TASK NO. 01 WORK UNIT ACCESSION NO

11. TITLE (Include Security Classification)
(U) Measurements of Atmospheric Transmission Through Falling Snow

12. PERSONAL AUTHOR(S)
Dr. A. Ben-Shalom and Dr. A. D. Devir

13a. TYPE OF REPORT	13b. TIME COVERED	14. DATE OF REPORT (Year, Month, Day)	15. PAGE COUNT
Final	FROM 1984 TO 1987	September 1987	34 + App. A & B

16. SUPPLEMENTARY NOTATION

17. COSATI CODES			18. SUBJECT TERMS (Continue on reverse if necessary and identify by block number)
FIELD	GROUP	SUB-GROUP	Atmospheric transmission, ~~during periods of~~ snowfall. Infrared and visible spectral regions, GREAT BRITAIN. (JES)
04	01		

19. ABSTRACT (Continue on reverse if necessary and identify by block number)

Measurements of atmospheric transmission during periods of snow fall were made in the infrared and the visible spectral region, during winters of 1984-1987. Two field experiments were carried out in Israel and one field experiment in West Germany. Results of these measurements are presented in the Final Report. The measured data and results are not sufficient for validation or correction of the various models.

20. DISTRIBUTION/AVAILABILITY OF ABSTRACT ☒ UNCLASSIFIED/UNLIMITED ☐ SAME AS RPT. ☒ DTIC USERS	21. ABSTRACT SECURITY CLASSIFICATION Unclassified
22a. NAME OF RESPONSIBLE INDIVIDUAL Jerry C. Comati	22b. TELEPHONE (Include Area Code) +441-402-7331 22c. OFFICE SYMBOL AMXSN-UK-RE

DD FORM 1473, 84 MAR — 83 APR edition may be used until exhausted. All other editions are obsolete

SECURITY CLASSIFICATION OF THIS PAGE
Unclassified

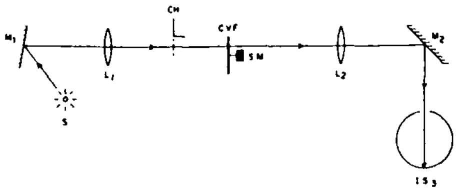

Fig. 1. Optical system for reflectance measurements in the VIS region: S, source; M_1,M_2, plane mirrors; L_1,L_2, lenses; IS_1, integrating sphere; CVF, circular variable filter.

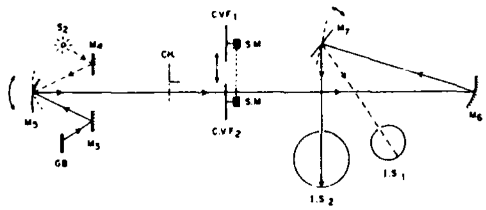

Fig. 2. Optical system for measurements in the infrared region (schematic): S_2, projector lamp; M_3,M_4,M_7, plane mirrors; M_5,M_6, spherical mirrors; GB, globar; IS_1, integrating sphere for the FIR region; IS_2, integrating sphere for the NIR region; CVF_1,CVF_2, circular variable filters.

standard was a plate coated with a diffuse gold coating. The integrating sphere IS_1 had a diameter of 5 cm and was coated with a diffuse gold coating provided by Labsphere, Inc. The detector was a Charles Reeder thermopile with a sensitive area of 6 × 6 mm and a time constant of 35 ms. The source was a globar operated at ~1600 K.

For the NIR region an integrating sphere IS_2 was built which operated by the Taylor III method and used the 7°/d configuration. Its diameter was 10 cm and it was coated with Eastman White Reflectance Coating, catalog No. 6080. A detailed description of this sphere will be given below. The source in this case was a 650-W projection lamp with a tungsten filament. The same Charles Reeder thermopile that was used in the FIR was also used here, and a chopper frequency of 13 Hz modulated the beam.

III. Taylor III Method

In this method two measurements are required to find the reflectance of the sample. In the first measurement the illuminating beam strikes the sample. In this mode the detector receives radiation from a portion of the sphere wall that is not directly illuminated by reflected radiation from the sample, although it is illuminated by secondary reflections from the surrounding walls. Figure 3 shows the small baffle that shields the sphere wall from the sample. The signal received from this measurement is called I_1. In the second measurement the sphere wall is illuminated directly by the beam entering the sphere, and there is no baffle between the illuminated portion and the area seen by the detector. This signal is called I_2. Sharp

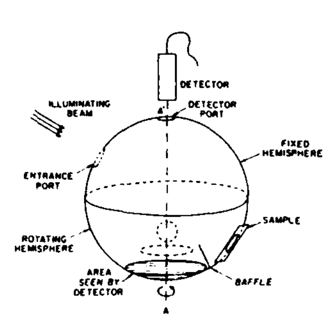

Fig. 3. Integrating sphere for absolute measurements of diffuse reflectance (schematic).

and Little[9] have shown that in this case the reflectance of the sample, ρ_1, is given to a first approximation by

$$\rho_1 = \frac{I_1}{I_2}\frac{A_0}{A_1 + A_2}, \qquad (1)$$

where A_0 is the total sphere wall area, A_1 is the area of the sample hole, and A_2 is the net area of the sphere wall. It should be emphasized, however, that this approximation holds only when the area of all the openings in the sphere is very small compared with A_0. More recently it has been shown by Budde and Dodd[7] that Eq. (1) also holds when finite openings are considered, but on the condition that

$$A_0 \gg A_1(\rho_1 - \rho_2), \qquad (2)$$

where ρ_2 is the reflectance of the sphere wall. If condition (2) does not hold, a different expression for ρ_1 may be derived. In this case, however, prior knowledge of ρ_2 is required. ρ_2 may be determined by measuring the reflectance of a sample identical with the sphere wall. In this case Eq. (1) holds rigorously.

Figure 3 is a schematic diagram of the sphere. It consists of an upper half, which is stationary, and a lower half, which can be rotated around a vertical axis AA'. At the center of the upper half there is a port through which the detector receives radiation from part of the sphere opposite the port (shaded in Fig. 3). The lower half contains a port for the sample. The baffle shields the part of the sphere wall viewed by the detector from the sample.

The reflectance is measured as follows: I_1 is measured by rotating the sphere until the sample is opposite the entrance port as shown in Fig. 3. The signal received in this portion is I_1. The lower half of the sphere is then rotated by ~90° until the illuminating beam falls on the sphere wall. In this position the sample port and the baffle are shown as dotted lines in Fig. 3. The area viewed by the detector is not shielded from the illuminated area on the sphere wall in this position. This yields the signal I_2. Equation (1) is now used to calculate the reflectance of the sample. It should be emphasized here that Eq. (1) is valid only when the sample and the sphere coating are completely diffuse and condition (2) is met. We tried to meet

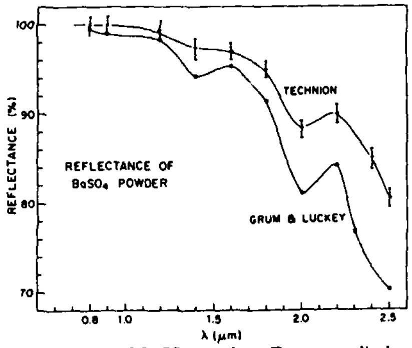

Fig. 4. Reflectance of $BaSO_4$ powder. Top curve displays the present results; bottom curve displays the results of Ref. 10.

Table I. Reflectance of $BaSO_4$ Powder Manufactured by Kodak, as Measured in the Reflectometer Laboratory by an Absolute Method and as Published Earlier in Ref. 10

λ(μm)	ρ_{abs}(%)	ρ(%) According to Ref. 10
0.8	100.0	99.6
1.0	100.0	99.1
1.2	99.5	98.3
1.4	97.5	93.2
1.6	97.0	94.4
1.8	95.0	91.5
2.0	88.5	81.1
2.2	90.0	84.2
2.4	85.0	76.8
2.5	81.0	70.3

substantial discrepancy for longer wavelengths which reached almost 11% at 2.5 μm.

Some of the sources for this discrepancy may be different degrees of contamination of the samples by adsorbed water, for example, or by other contaminants. Differences in the density of the samples may also contribute to the observed discrepancy. One might conclude in view of the different results, that this material is not as reliable in the role of a reflectance standard as might have been thought in the past.

VIII. Conclusion

A computer-controlled reflectometer was designed and built for the 0.4–13.5-μm region. The system utilized several integrating spheres. For the problematic 0.8–2.5-μm region, an absolute integrating sphere was constructed and good results were obtained for several standard materials. This system has been in use routinely for several years for reflectance measurement of many types of material of interest in the infrared.

The authors are grateful for the technical help of Shmuel Ariov who assisted in designing and constructing the integrating spheres and the reflectometer.

Dieter Clement is on leave from Forschunginstitut fur Optik, Schloss Kressbach, Tubingen, Federal Republic of Germany.

References

1. D. J. Lovell, "Theory and Applications of Integrating Sphere Technology," Laser Focus/Electrooptics, p. 86 (May 1981).
2. D. G. Goebel, "Generalized Integrating-Sphere Theory," Natl. Bur. Stand. U.S. Spec. Publ. 300, 473 (1971).
3. F. J. J. Clarke, "Measurment of the Radiometric Properties of Materials for Building and Aerospace Applications," Proc. Soc. Photo-Opt. Instrum. Eng. 24, 40 (1980).
4. F. Grum and T. E. Wightman, "Absolute Reflectance of Eastman White Reflectance Standard," Appl. Opt. 16, 2775 (1977).
5. W. Erb, "Requirements for Reflection Standards and the Measurement of Their Reflection Values," Appl. Opt. 14, 493 (1975).
6. W. H. Venable, Jr., J. J. Hsia, and V. R. Weidner, "Development of an NBS Reference Spectrophotometer for Diffuse Transmittance and Reflectance," Natl. Bur. Stand. U.S. Tech. Note 594-11 (1976).
7. W. Budde and C. X. Dodd, "Absolute Reflectance Measurements in the D/0° Geometry," Die Farbe 19, 94 (1970).
8. W. W. Wendlandt and H. G. Hecht, *Reflectance Spectroscopy* (Interscience, New York, 1966), Chap. 10, p. 254.
9. C. H. Sharp and W. F. Little, "Measurements of Reflection Factors," Trans. Illum. Eng. Soc. 15, 802 (1920).
10. F. Grum and G. W. Luckey, "Optical Sphere Paint and a Working Standard of Reflectance," Appl. Opt. 7, 2289 (1968).